The hysteresis loop of internal friction associated with magnetic flux pinning in $YBa_2Cu_3O_{7-x}$ superconductors

1992 J. Phys.: Condens. Matter 4 4519

(http://iopscience.iop.org/0953-8984/4/18/018)

J. Phys.: Condens. Matter 4 (1992) 4519–4526. Printed in the UK

The hysteresis loop of internal friction associated with magnetic flux pinning in $YBa_2Cu_3O_{7-x}$ superconductors

Y T Wen†, T S Kê†, H G Bohn‡, H Soltner‡ and W Schilling‡

† Laboratory of Internal Friction and Defects in Solids, Institute of Solid State Physics, Academia Sinica, Hefei 230031, People's Republic of China

‡ Institut für Festkörperforschung der Forschungszentrum, 5170 Jülich, Federal Republic of Germany

Received 28 August 1991, in final form 2 January 1992

Abstract. The hysteresis loops of internal friction associated with the magnetic flux pinning in high-T_c bulk and film $YBa_2Cu_3O_{7-x}$ superconductors were investigated by the vibrating-reed technique. When a cyclic magnetic field is applied, both the internal friction Q_B^{-1} and the resonant frequency f_r exhibit a hysteresis loop. This is explained on the basis of the Bean model. It is considered that the variation in the Q_B^{-1} hysteresis loop reflects the different mobilities of the flux lines at different positions of the pinning potential well. The critical current density J_c and the bulk pinning force density P_V were estimated from the Q_B^{-1} hysteresis loop for the film specimen.

1. Introduction

In 1986, the vibrating-reed technique was introduced for the study of magnetic flux pinning [1, 2]. Since then this technique has been successfully used to investigate the magnetic flux pinning for normal and high-T_c superconductors [3–8]. The experimental results presented by Gregory *et al* [9] demonstrated that the vibrating-reed technique is also suitable for the study of magnetic flux pinning of superconducting films.

Previous studies were concentrated on the measurement of the variation in internal friction Q^{-1} and resonant frequency f_r with temperature T and applied magnetic field B_a. In another paper [10], we reported the amplitude effect of the internal friction and resonant frequency.

Among the techniques for measuring the magnetic flux pinning of superconductors, an important method is the measurement of the hysteresis loop of magnetization. From this loop the pinning force and the critical current density can be obtained.

In this paper, we present the experimental results of the hysteresis loop of internal friction and resonant frequency measured when a cyclic magnetic field is applied. The variation in the loop with amplitude and maximum applied magnetic field was systematically studied.

2. *Experimental technique*

The experimental apparatus used is an electrostatically driven and modulated frequency-detected vibrating reed with a cryostat (10–300 K) and an electric magnet (0–1.5 T). The magnetic field is in the longitudinal direction of the vibrating reed.

0953-8984/92/184519+08$04.50

It is controlled by an IBM PC/AT computer. The vibration of the specimen at a constant amplitude is driven by a self-exciting loop. The amplitude A_m can be varied by gain adjustment of the loop and is given by an arbitrary unit with an error of about 5%. By estimation, $A_m = 1$ corresponds to an amplitude of about 100 nm.

The internal friction Q^{-1} and resonant frequency f_r were measured by the free-decay method. The precision of Q^{-1} is better than 1%. The precision of f_r depends on the magnitude of Q^{-1} and is better than $Q^{-1}/100$.

The internal friction can be expressed by

$$Q^{-1} = Q_0^{-1} + Q_B^{-1}$$

where Q_0^{-1} is the internal friction of the specimen itself and is called the background internal friction, and Q_B^{-1} is produced when a magnetic field is applied and is called the internal friction of magnetic flux pinning. The variation in the squared frequency is

$$\mathrm{d}f_r^2 = (f_r^2 - f_0^2)/f_0^2$$

where f_0 is the resonant frequency when $B_a = 0$.

A sintered $YBa_2Cu_3O_{7-x}$ superconductor was prepared by the solid phase reaction method. The size of the specimen is 15 mm × 2.5 mm × 0.24 mm. At room temperature, the resonant frequency $f_r \simeq 1.4$ kHz and the background internal friction $Q_0^{-1} \simeq 3 \times 10^{-3}$. The $YBa_2Cu_3O_{7-x}$ film specimen with $T_c = 90$ K was made by a DC sputtering method [11] on a single-crystal MgO substrate. The thickness of the film is 800 nm. The effective size of the vibrating reed for the film specimen is 6.5 mm × 3 mm × 0.23 mm. This smaller size gives a higher resonant frequency (about 10 kHz).

Before measuring the hysteresis loop of Q_B^{-1} and $\mathrm{d}f_r^2$, the cyclic magnetic field was applied several times so that a stable state of the flux lines was established in the specimen.

3. Experimental results

Figure 1 shows the magnetic hysteresis loop of the internal friction Q_B^{-1} and the resonant frequency $\mathrm{d}f_r^2$ for the sintered specimen. It is seen that the values of Q_B^{-1} and $\mathrm{d}f_r^2$ corresponding to descending B_a are larger than that corresponding to ascending B_a.

The hysteresis loop of Q_B^{-1} is complex.

(1) At first, Q_B^{-1} increases monotonically with increasing B_a.
(2) When B_a begines to decrease, Q_B^{-1} continues to increase to a maximum value.
(3) Then Q_B^{-1} decreases with decreasing B_a.
(4) When B_a decreases to zero, Q_B^{-1} becomes close to zero.

The loop of $\mathrm{d}f_r^2$ is simple. $\mathrm{d}f_r^2$ increases monotonically with increasing B_a and decreases when B_a decreases.

Figure 2 shows the hysteresis loops of Q_B^{-1} and $\mathrm{d}f_r^2$ for the film specimen. Similar to the case of the sintered specimen, Q_B^{-1} and $\mathrm{d}f_r^2$ with decreasing B_a are larger than those with increasing B_a. The shape of the $\mathrm{d}f_r^2$ loop is similar to that of

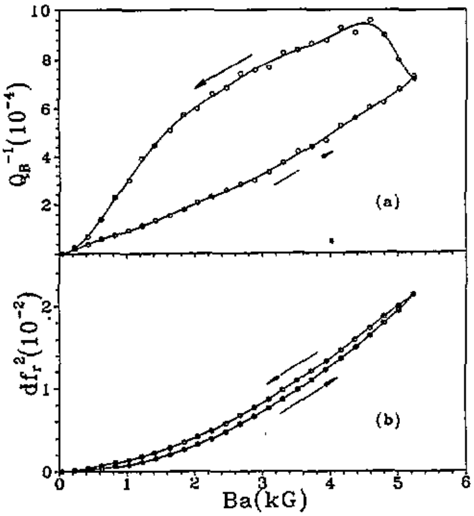

Figure 1. Hysteresis loops of Q_B^{-1} and $d f_r^2$ for the sintered specimen (T = 10 K; $A_m \simeq 3$). The arrows show the increasing and decreasing magnetic fields.

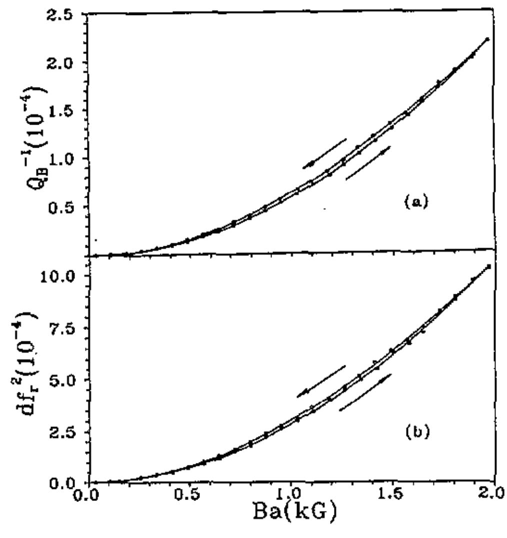

Figure 2. Hysteresis loops of Q_B^{-1} and $d f_r^2$ for the film specimen (T = 19.8 K). The arrows show the increasing and decreasing magnetic fields.

the sintered specimen. On the contrary, the Q_B^{-1} loop of the film specimen with decreasing B_a cannot be divided into several steps. The hysteresis loops of Q_B^{-1} and $d f_r^2$ are small with hysteresis values of B_a and Q_B^{-1} of only several tens of gausses and 10^{-6}, respectively.

It should be pointed out that Q_B^{-1} is strongly dependent on the amplitude A_m, and this will be reported in another paper [10].

Figure 3 shows a set of hysteresis loops of Q_B^{-1} with different amplitudes for the sintered specimen. At small A_m, the Q_B^{-1} has a large hysteresis area and exhibits several steps as described above. When A_m increases gradually, the level of the Q_B^{-1} loop drops, and the area of the loop decreases; the second step of the loop becomes small and finally disappears. When A_m is very large, the loop becomes very narrow. Thus the Q_B^{-1} loop of the sintered specimen is strongly dependent on A_m.

Figure 4 shows a set of hysteresis loops of $\mathrm{d}f_r^2$ with the same conditions as figure 3. When A_m varies from 1 to 16, there is no change in the shape and the level of the $\mathrm{d}f_r^2$ loop. Therefore, the $\mathrm{d}f_r^2$ loop is independent of A_m.

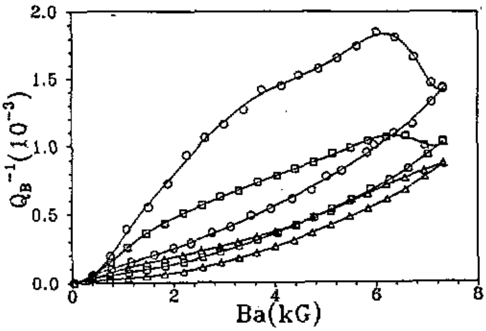

Figure 3. Amplitude effect of the Q_B^{-1} loop for the sintered specimen ($T = 13.4$ K; $B_{max} = 7.25$ kG): ○, $A_m = 1$; □, $A_m = 2.5$; △, $A_m = 16$. A_m is in arbitrary units.

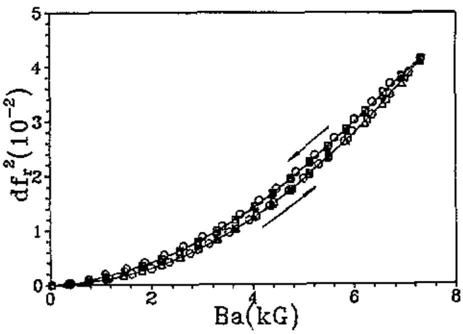

Figure 4. Amplitude effect of the $\mathrm{d}f_r^2$ loop for the sintered specimen. The conditions are the same as in figure 3. The arrows show the increasing and decreasing magnetic fields.

A change in A_m may change the dynamic distribution of the magnetic flux density in the superconductor. The amplitude effect of the Q_B^{-1} loop described above may reflect the fact that Q_B^{-1} is dependent not only on the applied magnetic field but also on the distribution of the magnetic flux density and the moving state of the magnetic flux lines in the pinning barrier. Then the hysteresis value of the Q_B^{-1} loop may reflect the gradient of the magnetic flux density. There is a larger gradient of the magnetic flux density when A_m is small.

Figure 5 shows a set of curves of Q_B^{-1} and $\mathrm{d}f_r^2$ for a sintered specimen for several maximum applied magnetic fields B_{max}. It is seen that the loops for smaller B_{max} are enclosed in the loops for larger B_{max}. When B_{max} is small, the Q_B^{-1} loop exhibits steps (1), (2) and (4). With increasing B_{max}, step (2) becomes larger and finally saturates, and step (3) appears gradually.

Let us define the variation in step (2) of the Q_B^{-1} loop as dQ_2^{-1}. Figure 6 shows the variation in dQ_2^{-1} with B_{max}. The variation in dQ_2^{-1} from zero to a saturated value reflects the fact that the flux lines gradually penetrate into the superconducting specimen.

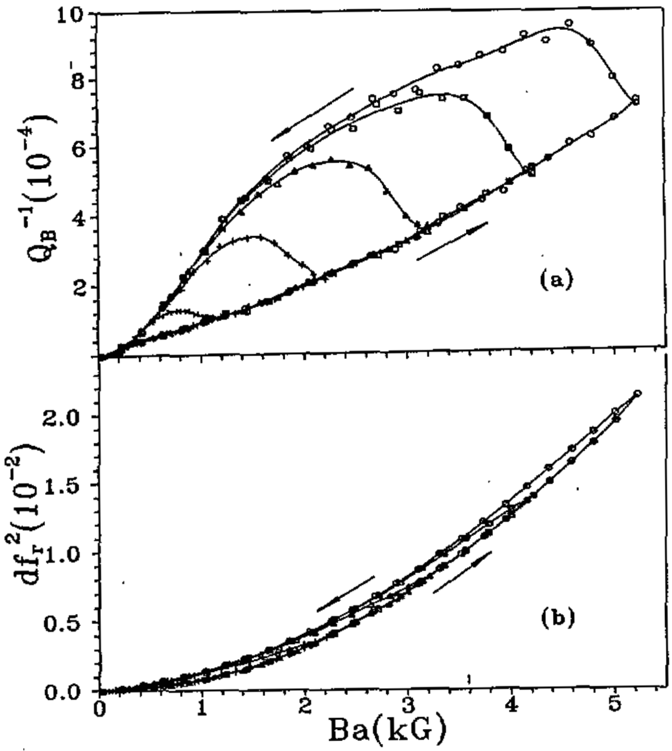

Figure 5. Hysteresis loops of Q_B^{-1} and df_r^2 with several B_{max} for the sintered specimen ($T = 33$ K; $A_m \simeq 1$). The arrows show the increasing and decreasing magnetic fields.

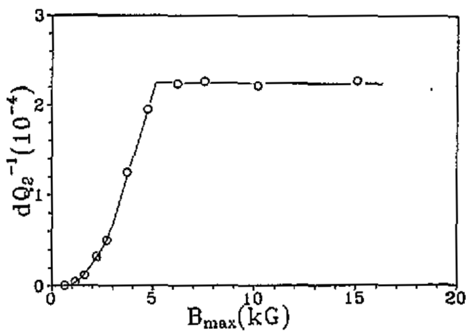

Figure 6. Plot of dQ_2^{-1} versus B_{max} for the sintered specimen ($T = 13.4$ K; $A_m \simeq 1$).

A set of Q_B^{-1} hysteresis loops for the film specimen was measured within the temperature range from 10 to 70 K. Assume dB to be the hysteresis value of the applied magnetic field corresponding to the same Q_B^{-1}. Figure 7 shows the relation between $\mathrm{d}B$ and the temperature T. The decrease in $\mathrm{d}B$ with increasing T reflects the fact that the pinning force decreases with increasing temperature.

4. Discussion

The Bean model has been widely applied to explain the results of electric and magnetic measurement of magnetic flux pinning. The distribution of the magnetic flux density inside the specimen has been generally considered to be linear as shown in figure 8. In figure 8, it can be seen that the areas under the line BA, indicating at B the distribution of the magnetic flux density on increasing magnetic field, and the line DC, indicating at D the distribution on decreasing magnetic field, are the same. Since this area is proportional to Q_B^{-1}, this means the same Q_B^{-1} value can be obtained by different increasing and decreasing applied magnetic fields corresponding to B and D which has the difference $\mathrm{d}B$ as indicated in figure 8. Therefore, the Bean model of linear distribution of magnetic flux density can aptly explain the Q_B^{-1} loop without step (2) as shown in figure 2(*a*) and figure 3. However, the situation is rather complex in the cases when step (2) occurs. It can be shown that in such cases the gradient of the distribution of magnetic flux density varies from the surface to the centre of the specimen. The displacement of the magnetic flux lines or the mobility of the flux lines during the vibration of the specimen is different in regions with different gradients of the distribution of magnetic flux density. In regions with smaller gradients, the flux lines lie near the centre of the pinning well. Then the mobility of flux lines is large, giving rise to a large energy dissipation. When the applied magnetic field begins to drop from its maximum value, regions with very small gradients will be created in the demarcation between the decreasing flux density and the flux density at the maximum magnetic field. The mobility of the flux lines is very large in such regions with very small gradients so that the energy dissipation is large. Consequently Q_B^{-1} increases when the applied magnetic field begins to drop from its maximum value and leads to the occurrence of step (2) in the Q_B^{-1} loop.

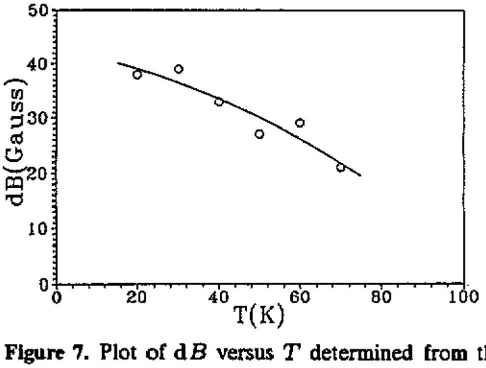

Figure 7. Plot of $\mathrm{d}B$ versus T determined from the Q_B^{-1} loops for the film specimen.

When the amplitude is large, the flux lines begin to depin in the course of increasing applied magnetic field so that the gradient of the distribution of flux density is correspondingly small. Consequently, when the applied magnetic field begins to

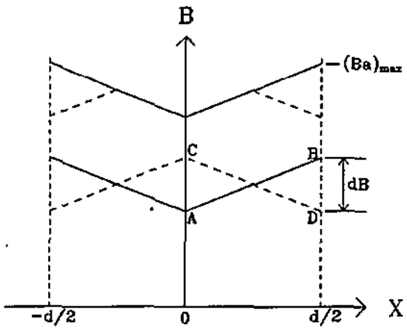

Figure 8. The Bean model with a linear distribution of magnetic flux density: ——, distribution of magnetic flux density with increasing applied magnetic field; – – –, distribution of magnetic flux density with decreasing applied magnetic field. d is the thickness of the film.

drop from its maximum value, the change in the gradient is small so that Q_B^{-1} will not increase at decreasing magnetic field and step (2) will not appear in the Q_B^{-1} loop.

Now let us calculate the critical current J_c and the volume pinning force density P_V from the hysteresis loop of Q_B^{-1}. The relation between J_c and the gradient $\partial B/\partial X$ of the magnetic flux density is

$$J_c = (1/\mu_0)(\partial B/\partial X)$$

where μ_0 is the vacuum permeability. Experimental data for the film specimen will be used in the calculation in order to avoid the difficulty introduced by the variation in $\partial B/\partial X$ at various locations in thicker specimens. The hysteresis value $\mathrm{d}B$ of the Q_B^{-1} loop is referred to the difference between the B_a values at increasing and decreasing magnetic fields giving the same Q_B^{-1} . Since $\mathrm{d}B$ varies with B_a, the value of $\mathrm{d}B$ used in the calculation is that corresponding to $(\mathrm{d}Q^{-1})_{max}$ which is the difference between the Q_B^{-1} values at decreasing and increasing magnetic fields. The linear extent corresponding to $\mathrm{d}B$ is one half of the specimen thickness, i.e. $d/2$ (figure 8). Thus we have

$$\partial B/\partial X \simeq \mathrm{d}B/(d/2)$$

and

$$J_c \simeq (1/\mu_0)[\mathrm{d}B/(d/2)].$$

The volume pinning force is given by

$$P_V = J_c B.$$

For estimation, B can be substituted by B_a.

From figure 7 which shows the temperature dependence of $\mathrm{d}B$ in the temperature range from 10 to 70 K, the J_c value estimated for the film specimen 800 nm thick varies from 8×10^9 to 4×10^9 A m^{-2} in this temperature range.

The assumption of a linear distribution of magnetic flux density is invalid for bulk specimens. Furthermore, the effect of particle size and the weak linking between particles on the Q_B^{-1} loop is not clear. Also the Q_B^{-1} loop then shows a strong amplitude effect. Further research is necessary for the clarification of all these problems.

Acknowledgment

This research has been partially subsidized by the National Natural Science Foundation of China (No 5880017).

References

[1] Brandt E H, Esquinazi P and Neckel H 1986 *J. Low Temp. Phys.* **63** 187
[2] Esquinazi P, Neckel H, Weiss G and Brandt E H 1986 *J. Low Temp. Phys.* **64** 1
[3] Brandt E H, Esquinazi P, Neckel H and Weiss G 1986 *Phys. Rev. Lett.* **56** 89
[4] Gupta A, Esquinazi P and Braun H F 1989 *Phys. Rev.* B **39** 12271
[5] Esquinazi P and Duran C 1988 *Physica* C **153** 1499
[6] Wen Y T, Xie C Y, Yuan L X, Kê T S, Qian Y T and Chen Z Y 1990 *Proc. 9th Int. Conf. on Internal Friction and Ultrasonic Attenuation in Solids* ed T S Kê (Beijing: International Academic Publishers) (Oxford: Pergamon) p 513
[7] Wen Y T, Xie C Y, Yuan L X, Kê T S, Qian Y T and Chen Z Y 1990 *J. Phys.: Condens. Matter* **2** 661
[8] Gammel P L, Schneemayer L F, Waszczak J V and Bishop D J 1988 *Phys. Rev. Lett.* **61** 1666
[9] Gregory S, Rogers C T, Venkatesan T, Wu X D, Inam A and Dutta B 1989 *Phys. Rev. Lett.* **62** 1548
[10] Wen Y T, Kê T S, Bohn H G, Soltner H and Schilling W 1992 *Physica* C at press
[11] Schubert J, Prieto P and Poppe U 1989 *Proc. 7th Int. Conf. on Ion- and Plasma-Assisted Techniques (Geneva)*